Polyhalogenation of isoflavonoids by the termite-associated *Actinomadura* sp. RB99

Seoung R. Lee,[a] Felix Schalk,[b] Jan W. Schwitalla,[b] René Benndorf,[b] John Vollmers,[c] Anne-Kristin Kastner,[c] Z. Wilhelm de Beer,[d] Minji Park,[e] Mi-Jeong Ahn,[f] Won Hee Jung,[e] Christine Beemelmanns,[,b] Ki-Hyun Kim[*, c]*

a) School of Pharmacy, Sungkyunkwan University, Suwon 16419, Republic of Korea E-mail: khkim83@skku.edu

b) Leibniz Institute for Natural Product Research and Infection Biology – Hans Knöll Institute (HKI), Beutenbergstraße 11a, 07745 Jena, Germany, E-mail: Christine.Beemelmanns@hki-jena.de

c) Institute for Biological Interfaces 5, Karlsruhe Institute of Technology, Hermann-von-Helmholtz-Platz 1, 76344 Eggenstein-Leopoldshafen, Germany

d) Department of Biochemistry, Genetics and Microbiology, Forestry and Agricultural Biotechnology Institute (FABI), University of Pretoria, Hatfield, 0083, Pretoria, South Africa

e) Department of Systems Biotechnology, Chung-Ang University, Anseong 17546, Republic of Korea

f) College of Pharmacy and Research Institute of Pharmaceutical Sciences, Gyeongsang National University, Jinju 52828, Republic of Korea

KEYWORDS: isoflavones, halogenation, symbiosis, metabolomics, Actinomadura.

ABSTRACT. Based on high-resolution tandem mass-spectrometry (HR-MS^2) and global natural products social molecular networking (GNPS), we found that plant-derived daidzein and genistein derivatives are polyhalogenated by a termite-associated *Actinomadura* species RB99. MS-guided purification of optimized growth conditions led to the isolation of eight polychlorinated isoflavones, including six novel derivatives, and seven novel polybrominated derivatives, two of which showed antimicrobial activity.

INTRODUCTION. Ecology-driven chemical analysis of microbial defensive symbionts in combination with omics-based dereplication strategies have revolutionized natural product chemistry and resulted in unprecedented discovery rates of newly identified bioactive natural products.[1-3] In particular, dissection of the delicate chemical interplay between microbes and farming insects has led to significant insights into the stability of symbiotic relations.[4]

Most prominently, farming insects, such as ants and termites that maintain a susceptible fungal monoculture in a nutritionally-rich environment (fungus comb) rely on protective symbiotic microorganisms to maintain the farming system and prevent detrimental infestations of the fungal garden.[5-7] However, it is still a conundrum that colonies of actively fungus-farming insects lack any signs of the presence of fungal contaminates or diseases. This suggests that the gut and comb environment, including the microbial community, provides effective defences against any incoming potentially parasitic and competitive species Amongst other bacterial lineages, Actinobacteria have been repeatedly shown to support farming life styles in many insect systems by acting as indirect defensive symbionts.[8,9] Based on the hypothesis that Actinobacteria contribute the well-being and protection of the fungus-farming termite *Macrotermes natalensis*,

we conducted phylogenetic and bioactivity studies of Actinobacteria derived from the termite colony, which clearly showed the bacterial diversity and metabolic capabilities of termite-associated bacterial species, actively secreting secondary metabolite mixtures that are active against co-occurring fungi and weed fungi.[6] We became particularly intrigued by members of the fairly underexplored genus *Actinomadura,*[8,10] most notable *Actinomadura* sp. RB99 (hence forward named RB99) as culture extracts showed antimicrobial activity against bacterial and fungal tests strains, but not against co-occuring weed fungi.[6] Metabolic investigations into RB99 resulted already in the isolation of a group of cyclic tripeptides, named natalenamides A-C,[11] and the polyketide fridamycin,[12] partially the cause of the observed antimicrobial activity of RB99.

In light of these ESI(-)-MS^2-driven exploratory studies, we became aware of the repeating occurrence of a MS^2 cluster that exhibited a characteristic peak patterns corresponding to polychlorinated metabolites. Here, we followed up on the halogenation ability of RB99 and report on the characterization of six novel poly-chlorinated, and seven novel poly-brominated isoflavones, two of which showed antimicrobial activity.

RESULTS AND DISCUSSION

Actinomadura sp. RB99 was grown on 100 ISP-2 agar plates as previously described (10 days, 30°C).[11,12] Methanolic culture extracts were subjected to solvent partitioning and analysed by high resolution tandem mass spectrometry (HR-MS^2). The acquired ESI(-)-MS^2 data was subjected to social molecular networking (GNPS) analysis. Analysis of the resulting MS-based datasets in combination with corresponding UV data resulted in the detection of a unique MS^2 cluster that exhibits characteristic peak patterns of polychlorinated metabolites with characteristic isoflavone-type UV signatures (Fig. 1 and S1). Dereplication of the detected HR-

MS data was performed using AntiBase[13] and SciFinder and revealed several so far not reported quasi-molecular ions, each of which correlated to a characteristic *m/z* halogenation pattern (Fig. S3-S8).

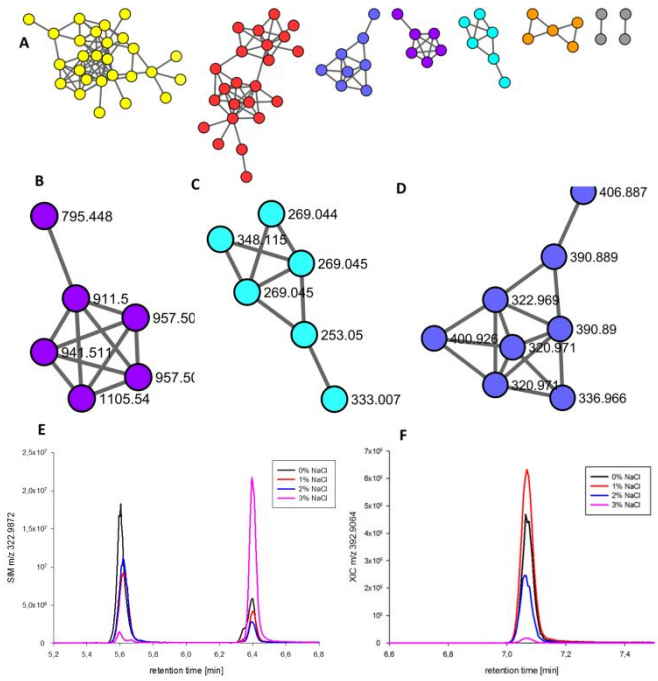

Figure 1. Global natural products social molecular networking analysis of HR-MS^2 of culture extracts derived from *Actinomadura* sp. RB99. (**A**) Selected section of GNPS-based analysis of methanolic culture extracts showing the most dominant detectable MS^2-cluster (negative ion trace). Based on public databases the following MS^2-clusters were assigned as (**B**) soyasapogenol derivatives, (**C**) isoflavonoids including daidzein or genistein and (**D**) polychlorinated isoflavonoids. Exemplary SIM of UHPLC-HESI-HRMS profiles at *m/z* $[M+H]^+$ 322.9872 ($C_{15}H_8O_4Cl_2$) (**E**) and 392.9093 ($C_{15}H_6O_4Cl_4$) (**F**).

The combined results were surprising at first as isoflavonoid-based natural products are typical-plant derived metabolites and biosynthesized via a biosynthetic branch of the

phenylpropanoid pathway.[14,15] Only few bacterial lineages, most notable *Streptomyces,* are able to produce the flavonoid naringenin; but subsequent conversion to isoflavones is unique to plants.[16-18] Based on our observations and previous reports,[19] it was quickly hypothesized that precursor isoflavones are likely derived from provided growth medium (ISP2) and then biotransformed by RB99 to polyhalogenated derivatives (Scheme 1).[20,21] Thus, we verified in a first step that isoflavones, such as daidzein and genistein are generally present in the applied standard growth medium by $HRMS^2$ and GNPS analysis (Fig. 1, Fig. S3). Both plant-derived metabolites were easily detectable in solid-phase extracts of sterile ISP2 medium and could be used for further transformation by RB99. We then analysed if supplementation of isoflavones, such as daidzein and genistein, and/or addition of salts (NaCl or KBr) to the culture broth of RB99 enhances the production of predicted halogenated isoflavone-containing metabolites (Fig. 1, Fig. S4-S8). In short, growth medium of RB99 (ISP2) was supplemented with varying concentrations of 1-3% NaCl, daidzein or genistein (0.5-10.0 mM), and combinations thereof. After cultivation for up to ten days, metabolites were extracted from the culture supernatant according to a generalized procedure and analysed using a standardized $HRMS^2$ analysis methods. First, we observed that supplementation of isoflavones daidzein or genistein reduced growth of RB99 significantly compared to growth in ISP2; bacterial growth was completely abolished when isoflavone concentrations exceeded 2.5 mM. Interestingly, addition of flavone naringenin resulted neither in reduced growth, nor in the formation of halogenated naringenins, nor in the increased formation of any other halogenated isoflavenoid. Only decreasing consumption of naringenin was observed by HRMS indicating that RB99 is able to degrade the plant metabolite.

We then tested growth and halogenation levels with varying NaCl concentrations. Cultures supplemented with 1% NaCl or 0.1% KBr showed normal growth behavior and an increase in the abundance of polychlorinated or polybrominated derivatives, respectively (Fig. S4-S8). NaCl concentrations exceeding 2% NaCl, however, resulted again in low biomass and metabolite production. Due to the stark variations in biomass and production titers of the diverse set of polyhalogenated derivatives across all experiments, a semi-quantitative correlation between biomass and degree of halogenation analysis was futile.

Then, we set out to characterize the predicted di-, tri- and tetra-halogenated isoflavones from culture broth of RB99 and performed preparative scale cultivations (6 L) on modified ISP2 broth (supplemented with either 1% NaCl or 0.1% KBr and additional 2 mg/L isoflavone (daidzein or genistein); 10 days, 30 °C, 150 rpm). Metabolite extraction was performed using a standard solid-phase extraction procedure.[11,12]

MS-guided purification of cultures supplemented with 1% NaCl resulted in the isolation of six new and two known polychlorinated derivatives (Fig. 2). First, maduraktermol A (**1**), was isolated and its molecular formula was determined to be $C_{15}H_8Cl_2O_4$ on the basis of a molecular ion peak at *m/z* 322.9873 $[M+H]^+$ (calcd for $C_{15}H_9Cl_2O_4$, 322.9872), which displayed a characteristic pseudo-molecular ion peak cluster at *m/z* 322.9873:324.9846:326.9832 $[M+H]^+$ with an approximate ratio of 9:6:1, suggesting the existence of two chlorine atoms in the molecule (^{35}Cl and ^{37}Cl, natural abundance about 3:1). The IR spectrum of **1** indicated the existence of aromatic ring (1590 cm^{-1}), carbonyl (1655 cm^{-1}), and hydroxyl (3445 cm^{-1}) functionalities, which correlated with distinct signals in the ^1H NMR spectrum (Table S4). The presence of signals δ_H 6.86 (1H, d, J = 2.0 Hz), 6.95 (1H, dd, J = 9.0, 2.0 Hz), 8.06 (1H, d, J =

9.0 Hz) was attributed to a 1,3,4-trisubstituted benzene ring and an additional signal at δ_H 7.52 (2H, s) indicated a 1,3,4,5-tetrasubstituted benzene.

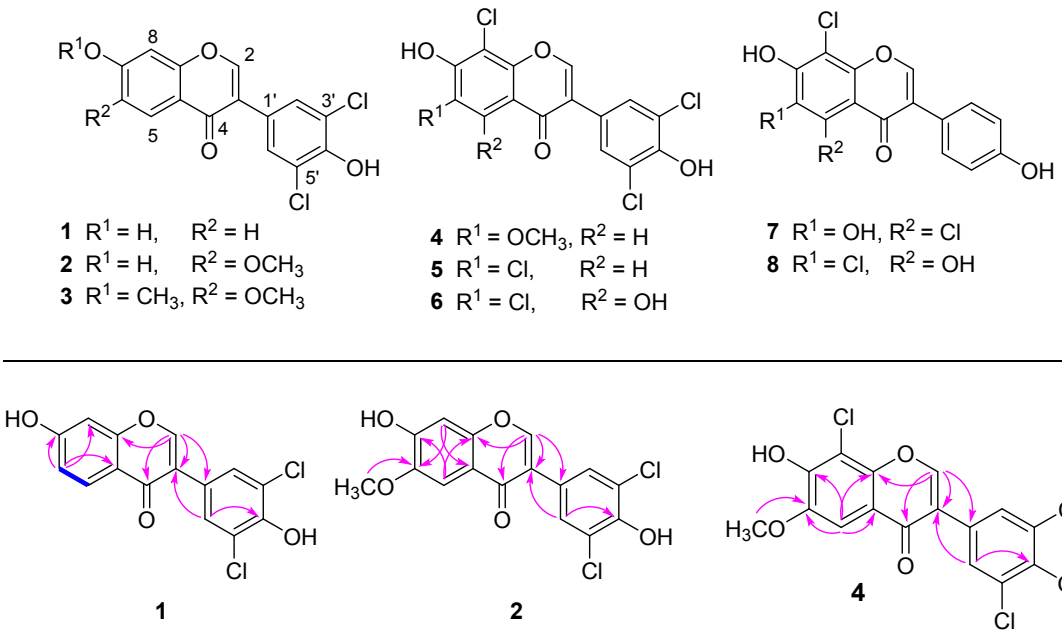

Figure 2. A) Chemical structures of isolated chlorinated compounds **1**-**8** and representative key COSY (blue bold line) and HMBC (pink arrow) correlations of **1, 2** and **4**.

Together with an isolated distinctive olefinic proton at δ_H 8.24 (1H, s), we deduced that **1** is built from an isoflavonoid scaffold, which was supported by a distinct flavonoid/isoflavonoid-type UV spectrum (λ_{max} 222, 250, and 298 nm). The ^{13}C NMR data of **1**, assigned based on the analysis of 2D NMR (^{1}H-^{1}H COSY, HSQC and HMBC) spectra, indicated the presence of 15 carbon signals (mostly aromatic), including one carbonyl group at δ_C 177.0. Comparative ^{1}H and ^{13}C NMR analysis using available in-house database and SciFinder confirmed that compound **1** closely resembled 3',4',5',7-tetrahydroxyisoflavone (Fig. 2) and was of symmetric nature [δ_H 7.52 (2H, s); δ_c 129.8 (C-2'/C-6')].[22] Thus, both chlorine atoms were assigned to non-protonated position C-3'/C-5'. Despite several attempts with varying NMR parameters no ^{13}C chemical shift

could be assigned to the chlorinated positions C-3'/C-5' most likely due to the nuclear quadrupole moment of Cl or the long relaxation time of these carbon atoms.

To determine the presence of two Cl atoms at C-3' and C-5' by heteronuclear correlations, HMBC experiments with varying coupling constants for ^{1}H-^{13}C (10 to 2 Hz) and ^{1}H-^{15}N (8 to 2 Hz) were conducted. Indeed, HMBC correlations of H-2' (δ_H 7.52)/C-3' (δ_C 124.0) and H-6'/C-5' could be confirmed when 3 and 4 Hz were applied to **1**, which led to confirmation of the chlorination at C-3' and C-5'. Overall, the chemical structure of **1** was determined as 3',5'-dichloro-4',7-dihydroxyisoflavone. Similar to the above described procedure, the structures of di, tri- and tetra-halogenated derivatives **2**-**6** were confirmed (see Electronic Supplementary Information (ESI)). While the chlorination pattern of compounds **1**-**5** was possible to assign based on comparative Ms and NMR analysis (Table 1 and 2), the position of the chlorine atoms in the A-ring of maduraktermol F (**6**) was ambiguous at first. Here, we used gauge-including atomic orbital (GIAO) NMR chemical shifts calculation at the B3LYP/6-31* level, followed by DP4 probability and correlation analysis (Fig. 3) to verify the chlorination pattern. Furthermore, we also isolated two known structural isomers (**7** and **8**) previously reported.[23]

Table 1. ^{1}H NMR (800 MHz) data of compounds **1-8** in MeOH-d_4.[a]

H	**1**	**2**	**3**	**4**	**5**	**6**	**7**	**8**
2	8.24, s	8.25, s	8.28, s	8.38, s	8.30, s	8.30, s	8.00, s	8.15, s
3								
4								
5	8.06, d (9.0)	7.56, s	7.57, s	7.55, s	8.03, s			
6	6.95, dd (9.0, 2.0)							
7								
8	6.86, d (2.0)	6.94, s	7.15, s					
9								
10								
1'								
2',6'	7.52, s	7.52, s	7.51, s	7.56, s	7.54, s	7.56, s	7.35, d (8.5)	7.38, d (8.5)
3',5'							6.83, d (8.5)	6.84, d (8.5)
4'								
6-OMe		3.96, s	3.94, s					
7-OMe			3.98, s					

[a] Coupling constants (in parentheses) are in Hz.

Table 2. ^{13}C NMR (200 MHz) data of compounds **1-8** in MeOH-d_4.[a,b]

C	**1**	**2**	**3**	**4**	**5**	**6**	**7**	**8**
2	155.1 d	154.7 d	154.7 d	154.8 d	154.7 d	155.1 d	153.0 d	155.0 d
3	124.7 s	123.1 s	123.5 s	123.1 s	123.1 s	122.8 s	124.9 s	124.9 s
4	177.0 s	177.1 s	177.0 s	176.5 s	176.0 s	180.5 s	180.6 s	181.9 s
5	128.3 d	104.5 d	105.0 s	103.0 d	124.9 d	n.d.	n.d.	n.d.
6	116.3 d	149.0 s	149.5 s	n.d.	n.d.	n.d.	n.d.	n.d.
7	164.7 s	156.2 s	156.4 s	151.7 s	161.7 s	n.d.	n.d.	n.d.
8	102.9 d	103.7 d	100.7 d	n.d.	n.d.	n.d.	n.d.	n.d.
9	159.5 s	154.5 s	154.0 s	150.1 s	154.2 s	152.8 s	153.5 s	152.7 s
10	117.8 s	117.1 s	118.2 s	117.1 s	124.6 s	n.d.	n.d.	n.d.
1'	124.9 s	124.9 s	124.5 s	124.6 s	124.4 s	122.1 s	123.8 s	122.4 s
2', 6'	129.8 d	129.8 d	129.7 d	129.8 d	129.9 d	129.9 d	131.2 d	131.3 d
3', 5'	124.0 d	n.d.	n.d.	n.d.	n.d.	n.d.	115.9 d	116.2 d
4'	150.4 s	151.6 s	152.5 s	150.4 s	150.5 s	150.6 s	158.6 s	159.0 s
6-OMe		56.2 q	56.2 q					
7-OMe			56.6 q					

[a]The assignments were based on HSQC, HMBC, and ^{1}H−^{1}H COSY experiments.
[b]Not detected (n.d.)

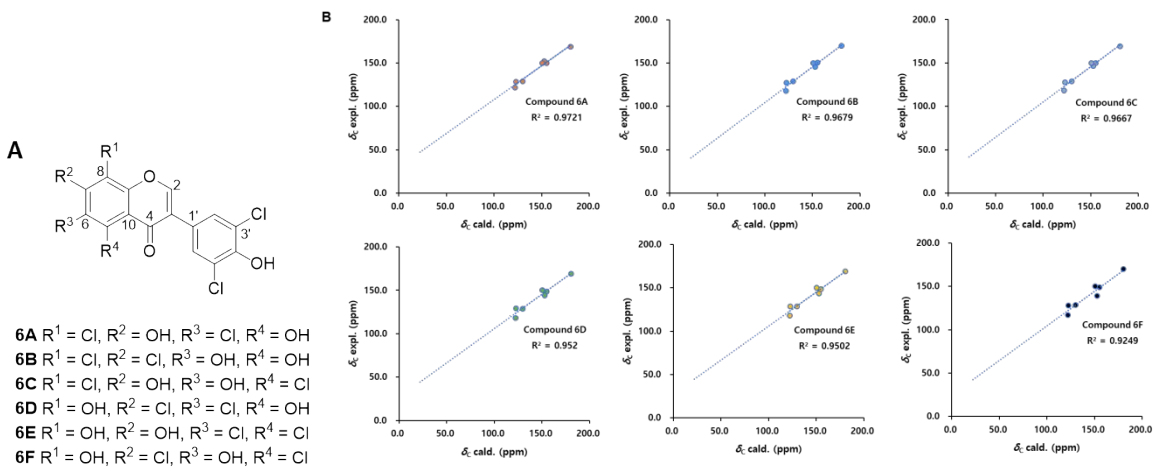

Figure 3. (A) Structures of most possible regioisomers (**6A-6F**). (B) Regression analysis of calculated versus experimental ^{13}C NMR chemical shifts for compounds **6** and the regioisomers **6A-6F**.

We then turned our focus on the MS-guided purification and analysis of culture medium supplemented with 0.1% KBr, which resulted in the identification of seven polybromiated derivatives **9-15**. First, derivative maduraktermol H (**9**), was isolated and its molecular formula was determined to be $C_{15}H_7Br_3O_4$ based on a protonated ion peak at *m/z* 488.7971 $[M+H]^+$ (Calcd for $C_{15}H_8Br_3O_4$, 488.7973), showed four pseudo-molecular ion peaks at *m/z* 488.7971:490.7951:492.7931:494.7912 with an approximate ratio of 1:3:3:1, suggesting the existence of three bromine atoms since bromine atom is present on nature in the ratio 1:1 of two isotropic forms (^{79}Br and ^{81}Br). The ^1H NMR spectrum of **9** displayed the presence of a 1,2,3,4-tetrasubstituted benzene ring at δ_H 7.00 (1H, d, J = 9.0 Hz), 8.00 (1H, d, J = 9.0 Hz) and a 1,3,4,5-tetrasubstituted benzene ring at δ_H 7.73 (2H, s), together with an isolated distinctive olefinic proton at δ_H 8.33 (1H, s). The ^{13}C NMR spectrum of **9** assigned by the aided of HSQC and HMBC experiments, exhibited 15 carbon resonances including 12 aromatic carbons

correlated above described units and additional carbonyl carbon at δ_C 176.9. Comparative 2D NMR data (^{1}H-^{1}H COSY, HSQC, and HMBC) of **9** afforded the confirmation of a polybrominated isoflavone. The locations of three bromine atoms were determined at C-8, C-3', and C-5' by HMBC correlations of H-6/C-8, H-2'/C-3', and H-6'/C-5' and the chemical structure of **9** was deduced as 3',5',8-tribromo-4',7-dihydroxyisoflavone. Using a similar analytical approach, structures of polybrominated derivatives **10-15** were characterized (Fig. 4, Table 3 and 4).

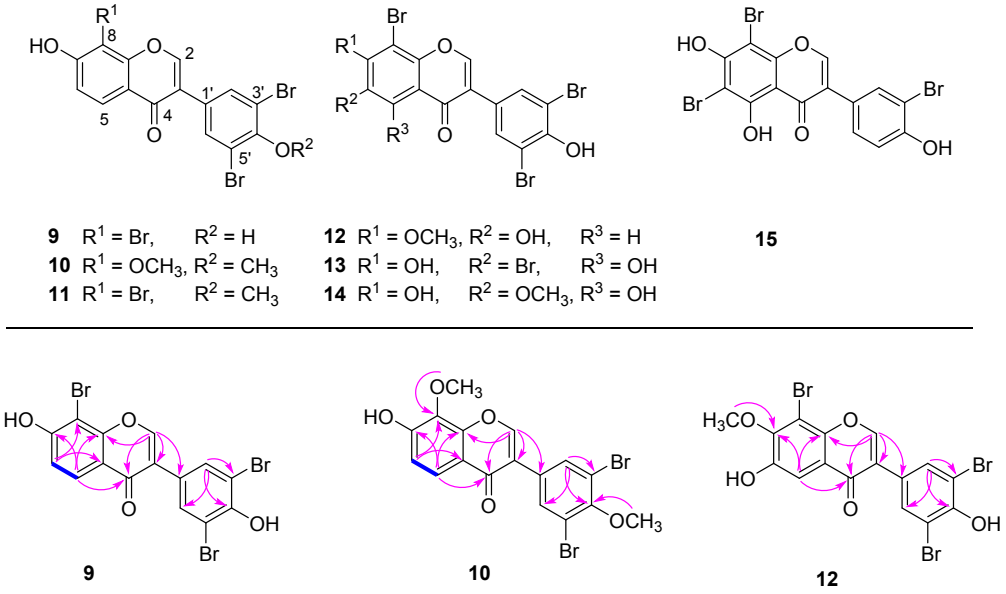

Figure 4. Chemical structures of isolated brominated compounds **9-15** and representative key COSY (blue bold line) and HMBC (pink arrow) correlations of **9, 10** and **12**.

Table 3. ^{1}H NMR (800 MHz) data of compounds **9-15**.[a]

H	**9**[b]	**10**[b]	**11**[c]	**12**[b]	**13**[c]	**14**[b]	**15**[b]
2	8.33 s	8.36 s	8.38 s	8.23 s	8.29 s	8.20 s	8.05 s
5	8.00 d (9.0)	7.80 d (9.0)	8.34 d (9.0)	7.41 s			
6	7.00 d (9.0)	7.00 d (9.0)	7.29 d (9.0)				
7							
8							
2'	7.73 s	7.83 s	8.09 s	7.72 s	8.05 s	7.72 s	7.70 d (2.0)
3'							
4'							
5'							6.95 d (8.0)
6'	7.73 s	7.83 s	8.09 s	7.72 s	8.05 s	7.72 s	7.35 dd (8.0, 2.0)
6-OMe						3.85 s	
7-OMe				3.92 s			
8-OMe		3.96 s					
4'-OMe		3.90 s	3.82 s				

[a] Coupling constants (in parentheses) are in Hz; [b] Spectroscopic data was acquired in MeOH-d_4; [c] Spectroscopic data was acquired in Pyridine-d_6.

Table 4. ^{13}C NMR (200 MHz) data of compounds **9-15**.[a]

C	**9**[b,c]	**10**[b,c]	**11**[b,d]	**12**[b,c]	**13**[d]	**14**[c]	**15**[c]
2	155.1 d	155.4 d	153.9 d	153.8 d	154.0 d	154.7 s	153.4 s
3	123.2 s	122.5 s	121.7 s	122.5 s	120.9 s	121.4 s	122.2 s
4	176.9 s	176.9 s	174.5 s	176.5 s	179.3 s	180.4 s	179.6 s
5	126.6 d	122.1 d	126.3 d	102.4 d	165.6 s	150.3 s	165.4 s
6	116.6 d	117.2 d	117.5 d	141.2 s	98.8 s	130.1 s	98.6 s
7	163.7 s	152.6 s	165.5 s	151.1 s	159.3 s	149.8 s	158.4 s
8	117.8 s	136.3 s	116.3 s	n.d.	103.9 s	100.9 s	102.3 s
9	156.3 s	152.6 s	155.8 s	152.6 s	154.6 s	150.3 s	155.1 s
10	98.4 s	117.9 s	98.9 s	124.4 s	91.0 s	89.8 s	91.4 s
1'	126.6 s	127.1 s	126.2 s	126.4 s	126.1 s	125.8 s	125.1 s
2'	133.7 d	134.2 d	133.7 d	133.6 d	133.7 d	133.7 d	134.5 d
3'	111.8 s	118.5 s	118.2 s	112.1 s	113.4 s	111.9 s	110.4 s
4'	152.9 s	154.9 s	154.0 s	152.9 s	153.2 s	152.6 s	155.2 s
5'	111.8 s	118.5 s	118.2 s	112.1 s	113.4 s	111.9 s	116.8 d
6'	133.7 d	134.2 d	133.7 d	133.6 d	133.7 d	133.7 d	130.3 d
6-OMe							
7-OMe				56.1 q		61.5 q	
8-OMe		61.5 q					
4'-OMe		60.8 q	60.6 q				

[a] Not detected (n.d.); [b] The assignments were based on HSQC, HMBC, and ^{1}H−^{1}H COSY experiments; [c] Spectroscopic data was acquired in MeOH-d_4; [d] Spectroscopic data was acquired in Pyridine-d_6.

Actinobacteria are well known for their capability to pursue biotransformations (reduction, hydroxylation, methylation and halogenation) of acquired substrates including isoflavones.[24-27] The observed modification pattern of isolated isoflavones suggests that RB99 is able to effectively halogenate the 3' and 5' position (ring B of daidzein and genistein), respectively.

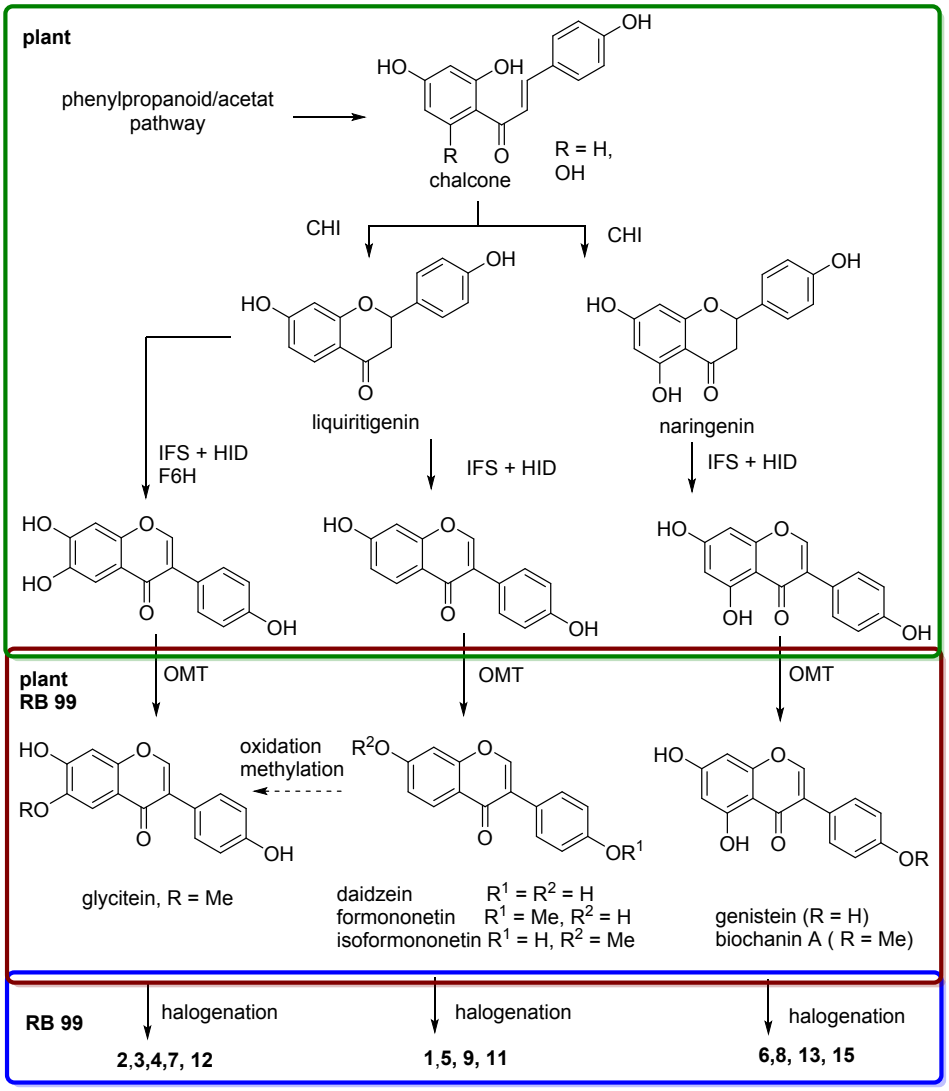

Scheme 1. Generalized biosynthesis of flavones and isoflavones in plants (green box), biotransformations in plants and/or RB99 (brown box), and only RB99 (blue box). (CHI = chalcone isomerase; IFS = 2-hydroxyisoflavanone synthase; HID = hydroxyisoflavanone

dehydratase, which produces the final isoflavone; F6H = flavanone 6-hydroxylase; OMT = O-methyl transferase.

Depending on the resulting substitution pattern of ring A, halogenation occurs *ortho* to hydroxyl or hydroxymethyl groups. However, timing and origin of hydroxylation/methylation and halogenation remains unknown (e.g. hydroxylation, methylation and halogenation) (Scheme 1). To identify candidate sequences that could be responsible for the observed halogenation (and/or oxidation and methylation), the genome of RB99 was sequenced using an Illumina NovaSeq using the paired-end approach (see, ESI). *De novo* genome assembly was performed using SPAdes v.3.13.1[28] and annotation was performed using Prokka v1.14.5 (Table S1, S2 and S8).[29,30] To identify putative halogenases, we performed a genome wide BLAST search of haloperoxidase peptide sequences using UniProt-Server.[31-33] We found several candidate genes that could be held accountable for the halogenation of isoflavones as homologous have been reported to be responsible for the halogenation of aromatic amino acids (Table S2 and S8).[34-36] The first putative candidate showed a high similarity based on peptide sequence (78.8%) with a non-haem bromo/chloroperoxidase CPO-A1 identified from *Kitasatospora aureofaciens (Streptomyces aureofaciens)* ATCC10762.[37] In addition, a putative FAD-dependent oxidoreductase was detected showing moderate similarities to two halogenases identified from *Actinoplanes sp. ATCC 53533* which are putatively involved in the chlorination of tyrosine residues.[38,39] Chloro and bromoperoxidases are well-known enzymes capable of halogenating a great variety of metabolites including activated aromatic compounds,[40,41] and current studies are directed towards analysing the putative haloperoxidases to determine the biosynthetic origin of halogenated isoflavones and to want extend the halogenation might serve as detoxification mechanism for RB99 in particular, and Actinobacteria in general.

As certain isoflavones were reported to have antibacterial activity,[17,18] we tested all halogenated isoflavones (**1–15**) for their growth inhibiting effects against human-pathogenic bacteria *Helicobacter pylori*, *Escherichia coli*, *Staphylococcus aureus*, and *Staphylococcus epidermidis*. Although, none of chlorinated derivatives showed antibacterial activity against *E. coli*, *S. aureus* and *S. epidermidis* (MIC > 100 μM), brominated derivatives **9** and **13** revealed a certain degree of selective growth inhibitory activity against *H. pylori* with MIC_{50} values of 72 μM [MIC of 12.5 μM] for compound **9** and >100 μM [MIC of 25 μM] for compound **13**, respectively (Table S3; positive control: metronidazole: MIC: 25 μM and MIC_{50}: 69 μM).

In conclusion, we found that two of the best studied isoflavones, daidzein and genistein,[17,18,20] both of which have been extensively studied for their ecological function in various plants and their potential role in human health,[42] are polyhalogenated by a termite-associated Actinomadura species. The biotransformation of bioactive plant metabolites into metabolites with altered, presumably less toxic bioactivity (detoxification process) by termite-associated Actinobacteria indicates towards an additional beneficial role of Actinobacteria within the termite's fungal garden microverse. Thus, this study guides exploration into the multiple functions of Actinobacteria within the termite system.

EXPERIMENTAL SECTION

General Experimental Procedures

IR spectra were acquired on a Bruker IFS-66/S FT-IR spectrometer. ESI and HR-ESI mass spectra were measured on a SI-2/LCQ DecaXP Liquid chromatography (LC)-mass spectrometer and UHPLC-HESI-HRMS measurements were performed on a Dionex Ultimate3000 system

combined with a Q-Exactive Plus mass spectrometer (Thermo Scientific) with a heated electrospray ion source (HESI). NMR spectra were recorded using a Varian UNITY INOVA 800 NMR spectrometer operating at 800 MHz (^{1}H) and 200 MHz (^{13}C), with chemical shifts given in ppm (δ). Preparative high-performance liquid chromatography (HPLC) utilized a Waters 1525 Binary HPLC pump with Waters 996 Photodiode Array Detector (Waters Corporation, Milford, CT, USA). Silica gel 60 (Merck, 230-400 mesh) and RP-C18 silica gel (Merck, 230-400 mesh) were used for column chromatography. Merck precoated Silica gel F254 plates and RP-18 F254s plates were used for thin layer chromatography (TLC). Semi-preparative HPLC used a Shimadzu Prominence HPLC System with SPD-20A/20AV Series Prominence HPLC UV-Vis Detectors (Shimadzu, Tokyo, Japan).

Metabolic Analysis

Analysis of halogenation pattern: For obtaining chlorinated derivatives, *Actinomadura* sp. RB99 was cultivated in 200 mL ISP2 broth for ten days at 30 °C at 150 rpm (preculture). Preculture was used to inoculate 500 mL ISP2 broth with adjusted NaCl concentration (1-5% NaCl). *Actinomadura* sp RB99 was cultivated for ten days at 30 °C at 150 rpm. Bacterial cells were harvested by centrifugation at 4000 x g for 10 min and the cell pellet and supernatant separated. The obtained supernatant was mixed with activated HP20 resin (40 g/L) and stirred at 4 °C overnight. The HP20 resin was separated by filtration, washed with ddH_2O (200 mL) and eluted using a MeOH/H_2O step gradient (unless stated otherwise: %MeOH refers to a mixture of MeOH and dH_2O). The collected MeOH eluent HP20 fractions were combined and dried under reduced pressure. Obtained extracts were re-suspended in corresponding %MeOH, centrifuged at 13000 x g for 10 min and adjusted to 5 mg/mL.

For obtaining brominated derivatives, a preculture (2 mL) of *Actinomadura* sp. RB99 was transferred to 100 mL ISP2 + 0.1% KBr and incubated for ten days at 30 °C (180 rpm). Bacterial cells were separated from culture supernatant by centrifugation (8000 x g, 10 min) and 10 mL 100% MeOH was added to yield a 10% MeOH culture supernatant. Metabolites from the supernatant were concentrated using an activated and equilibrated (10% MeOH). Chromabond C18ec cartridges filled with 500 mg of octadecyl-modified silica gel (Macherey-Nagel, Düren, Germany). Metabolites were eluted using a MeOH/H_2O step gradient and were concentrated in vacuo. The resulting extracts were adjusted with corresponding MeOH concentration to 5 mg/mL.

Large scale liquid cultivation: *Actinomadura* sp. RB99 was cultivated in 200 mL ISP2 broth for ten days at 30 °C at 150 rpm (preculture). Preculture was used to inoculate 6 L in ISP2 broth (+ 1% NaCl and 0.1 µM isoflavone), or 6 L ISP2 broth (+ 0.1% KBr and 0.1 µM isoflavone) for ten days at 30 °C at 150 rpm. Bacterial cells were harvested by centrifugation at 4000 x g for 10 min and the cell pellet separated. The obtained supernatant was mixed with activated HP20 resin (40 g/L) and stirred at 4 °C overnight. The HP20 resin was separated by filtration, washed with ddH_2O (2 L) and eluted using 50% MeOH (2 L) and 100% MeOH (2 L). The resulting MeOH-containing fractions were combined and concentrated *in vacuo*.

Chlorinated derivatives: Crude MeOH extract (20 g) was dissolved in distilled water (700 mL) and then solvent-partitioned with EtOAc (700 mL) three times, affording to 1.1 g of residue. The EtOAc-soluble fraction (1.1 g) was loaded onto a silica gel (230-400 mesh) column chromatography and eluted with a gradient solvent system of CH_2Cl_2-MeOH (100:1-1:1, v/v) provide to six fractions (A-F). Detailed inspection of LC/MS data of these six fractions with assistance of in-house UV spectral library suggested the existence of flavonoid or isoflavonoid

analogues displaying a specific UV pattern with unreported molecular formula. Fraction B (225 mg) was fractionated by preparative reversed-phase HPLC (Phenomenex Luna C18, 250 × 21.2 mm i.d., 5 μm) using CH_3CN-H_2O (2:8-1:0, v/v, gradient system, flow rate: 5 mL/min) to yield six subfractions (B1-B6). Subfraction B3 (20 mg) was separated by a semi-preparative reversed-phase HPLC (Phenomenex Luna C18, 250 × 10.0 mm i.d., 5 μm) with 61% MeOH/H_2O (isocratic system, flow rate: 2 mL/min) to afford compounds **1** (1.6 mg, t_R = 28.0 min), **2** (1.7 mg, t_R = 30.0 min), **3** (2.1 mg, t_R = 39.5 min), and **4** (1.9 mg, t_R = 61.0 min). Three subfractions (C1-C3) were acquired from fraction C (148 mg) utilizing preparative reversed-phase HPLC eluting CH_3CN-H_2O (2:8-9:1, v/v, gradient system, flow rate: 5 mL/min). Compound **7** (1.2 mg, t_R = 34.5 min) was isolated from subfraction C2 by semi-preparative reversed-phase HPLC with 65% MeOH/H_2O (isocratic system, flow rate: 2 mL/min). Subfraction C3 (10 mg) was separated by semi-preparative reversed-phase HPLC with 70% MeOH/H_2O (isocratic system, flow rate: 2 mL/min) to yield compounds **5** (2.0 mg, t_R = 35.5 min), **6** (1.7 mg, t_R = 44.0 min), and **8** (1.0 mg, t_R = 37.0 min).

Brominated derivatives: Crude MeOH extract (11 g) was dissolved in distilled water (700 mL) and solvent-partitioned with EtOAc (700 mL) three times, affording to 300 mg of residue. The EtOAc-soluble fraction (300 mg) was fractionated by preparative reversed-phase HPLC (Phenomenex Luna C18, 250 × 21.2 mm i.d., 5 μm) using CH_3CN-H_2O (3:7-1:0, v/v, gradient system, flow rate: 5 mL/min) to yield five subfractions (A-E). Subfraction C (15 mg) was separated by a semi-preparative reversed-phase HPLC (Phenomenex Luna C18, 250 × 10.0 mm i.d., 5 μm) with 64% MeOH/H_2O (isocratic system, flow rate: 2 mL/min) to afford compounds **9** (1.5 mg, t_R = 49.0 min), **12** (1.0 mg, t_R = 58.0 min), **13** (1.4 mg, t_R = 60.5 min), **14** (1.8 mg, t_R = 62.0 min), and **15** (1.0 mg, t_R = 64.0 min). Compounds **10** (1.2 mg, t_R = 25.0 min) and **11** (1.7

mg, t_R = 46.0 min) were purified by a semi-preparative reversed-phase HPLC (Phenomenex Luna C18, 250 × 10.0 mm i.d., 5 μm) with 74% MeOH/H_2O (isocratic system, flow rate: 2 mL/min).

Maduraktermol A (1): Yellowish gum; IR (KBr) ν_{max} 3445, 1655, 1590, 1513, 1225 cm^{-1}; UV (MeOH) λ_{max} (log ε) 200 (4.12), 222 (4.29), 250 (3.85), 298 (1.72) nm; ^1H (800 MHz) and ^{13}C (200 MHz) NMR data, see Table 1 and 2; HR-ESI-MS (positive-ion mode) *m/z* 322.9873 $[M+H]^+$ (Calcd. for $C_{15}H_9Cl_2O_4$, 322.9872).

Maduraktermol B (2): Yellowish gum; IR (KBr) ν_{max} 3443, 1650, 1585, 1510, 1213 cm^{-1}; UV (MeOH) λ_{max} (log ε) 200 (4.11), 223 (4.02), 260 (3.48), 326 (1.44) nm; ^1H (800 MHz) and ^{13}C (200 MHz) NMR data, see Table 1 and 2; HR-ESI-MS (positive-ion mode) *m/z* 352.9970 $[M+H]^+$ (Calcd. for $C_{16}H_{10}Cl_2O_5$, 352.9984).

Maduraktermol C (3): Yellowish gum; IR (KBr) ν_{max} 3451, 1670, 1594, 1517, 1219 cm^{-1}; UV (MeOH) λ_{max} (log ε) 200 (4.14), 223 (4.05), 260 (3.51), 325 (1.49) nm; ^1H (800 MHz) and ^{13}C (200 MHz) NMR data, see Table 1 and 2; HR-ESI-MS (positive-ion mode) *m/z* 367.0128 $[M+H]^+$ (Calcd. for $C_{17}H_{12}Cl_2O_5$, 367.0140).

Maduraktermol D (4): Yellowish gum; IR (KBr) ν_{max} 3548, 1692, 1611, 1535, 1241 cm^{-1}; UV (MeOH) λ_{max} (log ε) 206 (3.95), 266 (2.91), 320 (0.86) nm; ^1H (800 MHz) and ^{13}C (200 MHz) NMR data, see Table 1 and 2; HR-ESI-MS (positive-ion mode) *m/z* 386.9594 $[M+H]^+$ (Calcd. for $C_{16}H_9Cl_3O_5$, 386.9594).

Maduraktermol E (5): Yellowish gum; IR (KBr) ν_{max} 3422, 1616, 1577, 1501, 1216 cm^{-1}; UV (MeOH) λ_{max} (log ε) 205 (4.06), 257 (3.43), 318 (0.78) nm; ^1H (800 MHz) and ^{13}C (200 MHz) NMR data, see Table 1 and 2; HR-ESI-MS (positive-ion mode) *m/z* 390.9091 $[M+H]^+$ (Calcd. for $C_{15}H_6Cl_4O_4$, 390.9098).

Maduraktermol F (6): Yellowish gum; IR (KBr) ν_{max} 3430, 1643, 1524, 1138 cm^{-1}; UV (MeOH) λ_{max} (log ε) 208 (3.87), 269 (3.31) nm; ^{1}H (800 MHz) and ^{13}C (200 MHz) NMR data, see Table 1 and 2; HR-ESI-MS (positive-ion mode) *m/z* 406.9045 $[M+H]^+$ (Calcd. for $C_{15}H_6Cl_4O_5$, 406.9048).

Maduraktermol G (7): Yellowish gum; IR (KBr) ν_{max} 3428, 1617, 1509, 1119 cm^{-1}; UV (MeOH) λ_{max} (log ε) 206 (3.93), 267 (3.47) nm; ^{1}H (800 MHz) and ^{13}C (200 MHz) NMR data, see Table 1 and 2; HR-ESI-MS (positive-ion mode) *m/z* 338.9816 $[M+H]^+$ (Calcd. for $C_{15}H_9Cl_2O_5$, 338.9827)

Maduraktermol H (**9**)**:** Brownish gum; IR (KBr) ν_{max} 3435, 1631, 1580, 1510, 1202 cm^{-1}; UV (MeOH) λ_{max} (log ε) 209 (3.22), 232 (2.59), 252 (3.35), 301 (1.13) nm; ^{1}H (800 MHz) and ^{13}C (200 MHz) NMR data, see Table 3 and 4; HR-ESI-MS (positive-ion mode) *m/z* 488.7971 $[M+H]^+$ (Calcd for $C_{15}H_8Br_3O_4$, 488.7973).

Maduraktermol I (**10**)**:** Brownish gum; IR (KBr) ν_{max} 3410, 1627, 1552, 1501, 1235 cm^{-1}; UV (MeOH) λ_{max} (log ε) 208 (3.41), 234 (2.42), 257 (3.09), 309 (1.05) nm; ^{1}H (800 MHz) and ^{13}C (200 MHz) NMR data, see Table 3 and 4; HR-ESI-MS (negative-ion mode) *m/z* 452.8973 $[M-H]^-$ (Calcd for $C_{17}H_{11}Br_2O_5$, 452.8973).

Maduraktermol J (**11**)**:** Brownish gum; IR (KBr) ν_{max} 3410, 1692, 1573, 1513, 1203 cm^{-1}; UV (MeOH) λ_{max} (log ε) 209 (3.74), 221 (3.77), 232 (3.50), 253 (3.79), 309 (1.48) nm; ^{1}H (800 MHz) and ^{13}C (200 MHz) NMR data, see Table 3 and 4, respectively; HR-ESI-MS (positive-ion mode) *m/z* 502.8124 $[M+H]^+$ (Calcd for $C_{16}H_{10}Br_3O_4$, 502.8129).

Maduraktermol K (**12**)**:** Brownish gum; IR (KBr) ν_{max} 3589, 1702, 1628, 1543, 1270 cm^{-1}; UV (MeOH) λ_{max} (log ε) 210 (3.25), 265 (1.23), 327 (0.75) nm; ^{1}H (800 MHz) and ^{13}C (200

MHz) NMR data, see Table 3 and 4; HR-ESI-MS (positive-ion mode) *m/z* 518.8090 $[M+H]^+$ (Calcd for $C_{16}H_{10}Br_3O_5$, 518.8078).

Maduraktermol L (13): Brownish gum; IR (KBr) νmax 3403, 1593, 1511, 1104 cm-1; UV (MeOH) λmax (log ε) 212 (3.81), 243 (2.09), 271 (3.57) nm; 1H (800 MHz) and 13C (200 MHz) NMR data, see Table 3 and 4; HR-ESI-MS (negative-ion mode) m/z 580.6870 [M-H]- (Calcd for C15H5Br4O5, 580.6870).

Maduraktermol M (14): Brownish gum; IR (KBr) νmax 3420, 1611, 1528, 1121 cm-1; UV (MeOH) λmax (log ε) 210 (3.68), 243 (1.91), 271 (3.39) nm; 1H (800 MHz) and 13C (200 MHz) NMR data, see Table 3 and 4; HR-ESI-MS (negative-ion mode) m/z 532.7869 [M-H]- (Calcd for C16H8Br3O6, 532.7871).

Maduraktermol N (15): Brownish gum; IR (KBr) ν_{max} 3412, 1605, 1517, 1125 cm^{-1}; UV (MeOH) λ_{max} (log ε) 206 (3.96), 240 (2.13), 271 (3.87) nm; ^1H (800 MHz) and ^{13}C (200 MHz) NMR data, see Table 3 and 4; HR-ESI-MS (positive-ion mode) *m/z* 502.7762 $[M-H]^-$ (Calcd for $C_{15}H_6Br_3O_5$, 502.7765).

ASSOCIATED CONTENT

Supporting Information. The following file is available free of charge and contains information about fermentation and isolation procedures, analytical and spectral data (file type, PDF)

AUTHOR INFORMATION

Corresponding Author

Prof. Ki-Hyun Kim, School of Pharmacy, Sungkyunkwan University, Suwon 16419, Republic of Korea; E-mail: khkim83@skku.edu

Dr. Christine Beemelmanns, Leibniz Institute for Natural Product Research and Infection Biology – Hans Knöll Institute (HKI), Beutenbergstraße 11a, 07745 Jena, Germany, E-mail: Christine.Beemelmanns@hki-jena.de

Author Contributions

The manuscript was written through contributions of all authors. All authors have given approval to the final version of the manuscript.

Funding Sources

This work was supported by the National Research Foundation of Korea (NRF) grant funded by the Korean government (MSIT) (2018R1A2B2006879); the International Leibniz Research School for Microbial and Biomolecular Interactions (ILRS), the School for Microbial Communication (JSMC, DFG), the Deutsche Forschungsgemeinschaft (DFG, German Science Foundation) (BE 4799/3-1, CRC1127 project A6) and Project-ID 390713860 "Balance of the Microverse," (Germany's Excellence Strategy, EXC 2051)

Notes

There are no conflicts to declare.

ACKNOWLEDGMENT

We thank Louisa Hansske-Braun and Stefan Kuschke for assisting in the cultivation and solid phase extraction experiments.

.REFERENCES

1. M. Molloy, C. Hertweck, Antimicrobial Discovery Inspired by Ecological Interactions, *Curr. Opin. Microbiol*. 2017, **39**, 121–127.

2. H. Machado, R. N. Tuttle, P. R. Jensen, Omics-based Natural Product Discovery and the Lexicon of Genome Mining, *Curr. Opin. Microbiol*. 2017, **39**, 136–142.

3. T. Aron, E. C. Gentry, K. L. McPhail, L. F. Nothias, M. Nothias-Esposito, A. Bouslimani, D. Petras, J. M. Gauglitz, N. Sikora, F. Vargas, J. J. J. van der Hooft, M. Ernst, K. B. Kang, C. M. Aceves, A. M. Caraballo-Rodríguez, I. Koester, K. C. Weldon, S. Bertrand, C. Roullier, K. Sun, R. M. Tehan, P. C. A. Boya, M. H. Christian, M. Gutiérrez, A. M. Ulloa, J. A. Tejeda Mora, R. Mojica-Flores, J. Lakey-Beitia, V. Vásquez-Chaves, Y. Zhang, A. I. Calderón, N. Tayler, R. A. Keyzers, F. Tugizimana, N. Ndlovu, A. A. Aksenov, A. K. Jarmusch, R. Schmid, A. W. Truman, N. Bandeira, M. Wang, P. C. Dorrestein, Reproducible molecular networking of untargeted mass spectrometry data using GNPS, *Nat. Protoc.* 2020, https://doi.org/10.1038/s41596-020-0317-5

4. Beemelmanns, H. G. Guo, M. Rischer, M. Poulsen, Natural Products From Microbes Associated With Insects, *Beilstein J. Org. Chem*. 2016, **12**, 314–327.

5. A. Visser, T. Nobre, C. R. Currie, D. K. Aanen, M. Poulsen, Exploring the Potential for Actinobacteria as Defensive Symbionts in Fungus-Growing Termites, *Microb. Ecol*. 2012, **63**, 975–985.

6. T. R. Ramadhar, C. Beemelmanns, C. R. Currie, J. Clardy, Bacterial Symbionts in Agricultural Systems Provide a Strategic Source for Antibiotic Discovery, *J. Antibiot. (Tokyo), 2014,* **67**, 53-58.

7. E. B. Van Arnam, C. R. Currie, J. Clardy, Defense Contracts: Molecular Protection in Insect-Microbe Symbioses, *Chem. Soc. Rev*. 2018, **47**, 1638-1651.

8. R. Benndorf, H. Guo, E. Sommerwerk, C. Weigel, M. Garcia-Altares, K. Martin, H. Hu, M. Kuefner, Z. W. de Beer, M. Poulsen, C. Beemelmanns, Natural Products From Actinobacteria Associated With Fungus-Growing Termites, *Antibiotics 2018,* **7**, E83.

9. Beemelmanns, T. R. Ramadhar, K. H. Kim, J. L. Klassen, S. Cao, T. P. Wyche, Y. Hou, M. Poulsen, T. S. Bugni, C. R. Currie, J. Clardy, Macrotermycins A-D, Glycosylated Macrolactams From a Termite-Associated *Amycolatopsis* sp. M39, *Org. Lett.* 2017, **19**, 1000-1003.

10. H. Guo, R. Benndorf, D. Leichnitz, J. L. Klassen, J. Vollmers, H. Görls, M. Steinacker, C. Weigel, H. M. Dahse, A. K. Kaster, Z. W. de Beer, M. Poulsen, C. Beemelmanns, Isolation, Biosynthesis and Chemical Modifications of Rubterolones A-F: Rare Tropolone Alkaloids From Actinomadura Sp. 5-2, *Chem. Eur. J.* 2017, **23**, 9338-9345.

11. R. S. Lee, D. Lee, J. S. Yu, R. Benndorf, S. Lee, D. S. Lee, J. Huh, Z. W. de Beer, Y. H. Kim, C. Beemelmanns, K. S. Kang, K. H. Kim, Natalenamides A-C, Cyclic Tripeptides From the Termite-Associated *Actinomadura* sp. RB99, *Molecules* 2018, **23**, E3003.

12. S. Y. Yoon, S. R. Lee, J. Y. Hwang, R. Benndorf, C. Beemelmanns, S. J. Chung, K. H. Kim, Fridamycin A, a Microbial Natural Product, Stimulates Glucose Uptake Without Inducing Adipogenesis, *Nutrients* 2019, **11**, E765.

13. H. Laatsch, Antibase Version 5.0 - The Natural Compound Identifier. Wiley-VCH Verlag GmbH & Co. KGaA, **2017**; https://sso.cas.org

14. S. Horinouchi, Combinatorial Biosynthesis of Plant Medicinal Polyketides by Microorganisms, *Curr. Opin. Chem. Biol.* 2009, **13**, 197-204.

15. R. Alvarez-Alvarez, A. Botas, S. M. Albillos, A. Rumbero, J. F. Martín, P. Liras, Molecular Genetics of Naringenin Biosynthesis, a Typical Plant Secondary Metabolite Produced by Streptomyces Clavuligerus, *Microb. Cell. Fact*. 2015, **14**, 178.

16. O. Yu, J. Shi, A. O. Hession, C. A. Maxwell, B. McGonigle, J. T. Odell, Metabolic Engineering to Increase Isoflavone Biosynthesis in Soybean Seed, *Phytochemistry* 2003, **63**, 753-763.

17. N. Al-Maharik, Isolation of Naturally Occurring Novel Isoflavonoids: An Update, Nat. Prod. Rep, 2019, **36**, 1156-1195.

18. Q. Wang, X. Ge, X. Tian, Y. Zhang, J. Zhang, P. Zhang, Soy Isoflavone: The Multipurpose Phytochemical (Review), *Biomed. Rep*. 2013, **1**, 697-701.

19. H. J. Wang, P. A. Murphy, Isoflavone Content in Commercial Soybean Foods, *J. Agric. Food Chem*. 1994, **42**, 1666-1673; b) J. Reynaud, D. Guilet, R. Terreux, M. Lussignol,

and N. Walchshofer, Isoflavonoids in non-leguminous families: an update, Nat. Prod. Rep. 2005, **22**, 504-515.

20. J. R. Velandia, M. G. De Carvalho, R. Braz-filho, Novel Trichloro- and Tetrachloroisoflavone Isolated from Ouratea Semiserrta, *Nat. Prod. Lett.* 1998, **12**, 191-198.

21. J. M. Weber, A. R. Reeves, R. Seshadri, W. H. Cernota, M. C. Gonzalez, D. L. Gray, R. K. Wesley, Biotransformation and Recovery of the Isoflavones Genistein and Daidzein From Industrial Antibiotic Fermentations, *Appl. Microbiol. Biotechnol*. 2013, **97**, 6427-6437.

22. K. Nishiyama, S. Esaki, I. Deguchi, N. Sugiyama, S. Kamiya, Syntheses of Isoflavones and Isoflavone Glycosides, and Their Inhibitory Activity Against Bovine Liver β-Galactosidase, *Biosci. Biotech. Biochem*. 1993, **57**, 107-114.

23. O. Anyanwutaku, E. Zirbes, J. P. N. Rosazza, Isoflavonoids from Streptomycetes: Origins of Genistein, 8-Chlorogenistein, and 6,8-Dichlorogenistein, *J. Nat. Prod*. 1992, **55**, 1498-1504.

24. G. T. Maatooq, J. P. Rosazza, Metabolism of daidzein by Nocardia species NRRL 5646 and Mortierella isabellina ATCC 38063, *Phytochemistry* 2005, **66**, 1007-1011.

25. A. Chemler, E. Leonard, M. A. Koffas, *Flavonoid Biotransformations in Microorganisms. Anthocyanins*, 2008, New York: Springer, pp 191-255.

26. M. Hosny, J. P. N. Rosazza, Microbial Hydroxylation and Methylation of Genistein by Streptomycetes, *J. Nat. Prod*. 1999, **62**, 1609-1612.

27. H. R. Kang, D. Lee, R. Benndorf, W. H. Jung, C. Beemelmanns, K. S. Kang, K. H. Kim, Termisoflavones A–C, Isoflavonoid Glycosides from Termite-Associated Streptomyces sp. RB1, *J. Nat. Prod.* 2016, **79**, 3072-3078.

28. Bankevich, S. Nurk, D. Antipov, A. A. Gurevich, M. Dvorkin, A. S. Kulikov, V. M. Lesin, S. I. Nikolenko, S. Pham, A. D. Prjibelski, A. V. Pyshkin, A. V. Sirotkin, N. Vyahhi, G. Tesler, M. A. Alekseyev, P. A. Pevzner, SPAdes: A New Genome Assembly Algorithm and Its Applications to Single-Cell Sequencing, *J. Comput. Biol*. 2012, **19**, 455.

29. T. Seemann, Prokka: rapid prokaryotic genome annotation, *Bioinformatics* 2014, **30**, 2068.

30. Whole Genome Shotgun project has been deposited at DDBJ/ENA/GenBank under the accession RJNA596630P. The genome has been deposited at NCBI under the Accession JABMCA000000000. The version described in this paper is version 1.

31. https://www.uniprot.org/

32. M. C. R. Rranssen, Halogenation and Oxidation Reactions with Haloperoxidases, *Biocatalysis* 1994, **10**, 87-111.

33. M. Le Roes-Hill, N. Khan, S. G. Burton, Actinobacterial Peroxidases: an Unexplored Resource for Biocatalysis, *Appl. Biochem. Biotechnol*. 2011, **164**, 681-713.

34. T. Dairi, T. Nakano, K. Aisaka, R. Katsumata, M. Hasegawa, Cloning and Nucleotide Sequence of the Gene Responsible for Chlorination of Tetracycline, *Biosci. Biotechnol. Biochem*. 1995, **59**, 1099-1106.

35. K. Hubbard, C. T. Walsh, Vancomycin Assembly: Nature's Way, *Angew. Chem. Int. Ed. Engl.* 2003, **42**, 730-765.

36. B. Hofmann, S. Tölzer, I. Pelletier, J. Altenbuchner, K. H. van Pée, H. J. Hecht, Structural Investigation of the Cofactor-Free Chloroperoxidases, *J. Mol. Biol*. 1998, **279**, 889-900.

37. M. Weng, O. Pfeifer, S. Krauss, F. Lingens, K. H. van Pée, Purification, Characterization and Comparison of Two Non-Haem Bromoperoxidases From Streptomyces Aureofaciens ATCC 10762, *J. Gen. Microbiol*. 1991, **137**, 2539-2546.

38. T. L. Li, F. Huang, S. F. Haydock, T. Mironenko, P. F. Leadlay, J. B. Spencer, Biosynthetic Gene Cluster of the Glycopeptide Antibiotic Teicoplanin: Characterization of Two Glycosyltransferases and the Key Acyltransferase, *Chem. Biol*. 2004, **11**, 107-119.

39. P. Yaipakdee, L. W. Robertson, Enzymatic Halogenation of Flavanones and Flavones, *Pytochemistry* 2001, **57**, 341-347.

40. H. Yamada, N. Itoh, Y. Izumi, Chloroperoxidase-catalyzed Halogenation of Trans-Cinnamic Acid and Its Derivatives, *J. Biol. Chem*. 1985, **260**, 11962-11969.

41. H. Hong, M. R. Landauer, M. A. Foriska, G. D. Ledney, Antibacterial Activity of the Soy Isoflavone Genistein, *J. Basic Microbiol*. 2006, **46**, 329-335.

42. Spagnuolo, G. L. Russo, I. E. Orhan, S. Habtemariam, M. Daglia, A. Sureda, S. F. Nabavi, K. P. Devi, M. R. Loizzo, R. Tundis, S. M. Nabavi, Genistein and Cancer: Current Status, Challenges, and Future Directions, *Adv. Nutr*. 2015, **6**, 408-419.